2011 American Control Conference
on O'Farrell Street, San Francisco, CA, USA
June 29 - July 01, 2011

Symbolic Dynamic Filtering of Seismic Sensors for Target Detection and Classification★

Xin Jin† Shalabh Gupta† Asok Ray† Thyagaraju Damarla‡
xuj103@psu.edu szg107@psu.edu axr2@psu.edu rdamarla@arl.army.mil

Abstract— **Seismic sensors are widely used to monitor human activities, such as pedestrian motion and detection of intruders in a secure region. This paper presents a symbolic dynamics-based method of data-driven pattern classification by extracting the embedded information from noise-contaminated sensor time series. In the proposed method, the wavelet transforms of sensor data are partitioned to construct symbol sequences. Subsequently, the relevant information is extracted via construction of probabilistic finite state automata (PFSA) from symbol sequences. The patterns are derived from individual PFSA and are subsequently classified to make decisions on target classification. The proposed method has been validated on field data from seismic sensors to monitor infiltration of humans, light vehicles, and animals. The results of pattern classification demonstrate low false-alarm/missed-detection rate in target detection and high rate of correct target classification.**

Index Terms— **Personnel detection, time series analysis, feature extraction, continuous wavelet transform, symbolic dynamics, probabilistic finite state automata, seismic sensor**

I. Introduction

Unattended ground sensors (UGS) are widely used in industrial monitoring and military operations. Such UGS are usually lightweight devices that automatically monitor the activities at a site, and transfer target detection and classification reports to some higher level processing center. Commercially available UGS systems make use of multiple sensing modalities (e.g., acoustic, seismic, passive infrared, magnetic, electrostatic, and video). Efficacy of UGS systems is often limited by high false alarm rates because the onboard data processing algorithms may not be able to correctly discriminate different types of targets (e.g., humans from animals) [1]. Acoustic and seismic sensors are the most common modalities used in UGS systems. In this paper, seismic sensors are chosen for target detection and classification because they are less sensitive to Doppler effects (e.g., noise originating from moving vehicles), and atmospheric and terrain variations, as compared to acoustic sensors [2].

In a target detection and classification problem, the targets usually include human, vehicles, and animals. Discriminating human footstep signals from other targets and noise sources is a challenging problem, because the signal to noise ratio (SNR) of footsteps decreases rapidly with the distance between the sensor and the pedestrian. Furthermore, the footstep signals vary greatly for different persons and environments. Recent literature has shown detection of heavy vehicles that radiate loud signatures [3]. However, the signatures of humans and light vehicles are usually weak and contaminated with the sensor noise.

Current target detection methods using seismic signals can be classified into three categories: (i) time domain methods [4], (ii) frequency domain methods [3], [5], and (iii) time-frequency domain methods [2], [6]. Generally, time-domain analysis may not be able to perform very accurate target detection because of the interfering noise, complicated signal waveforms, and variations of the terrain [2]. However, these methods are limited by noise sources that might generate spikes or intermittent peaks in the data. Recent research has relied on either frequency-domain or time-frequency domain methods for target detection and classification. Specifically, wavelet transform-based methods have been useful for signal analysis because of their denoising and time-frequency localization properties.

The work reported here makes use of a wavelet-based feature extraction method, called Symbolic Dynamic Filtering (SDF) [7]. In SDF, transformed time series data are partitioned for conversion into symbol sequences. Subsequently, probabilistic finite-state automata (PFSA) are constructed from these symbol sequences to compress the pertinent information into low-dimensional statistical patterns. The SDF-based feature extraction algorithm mitigates the noise by using wavelet analysis, captures the essential signatures from the time-frequency domain of the signals, and generates low-dimensional feature vectors for pattern classification. Rao et al. [8] have reported a comparison of SDF with other statistical pattern tools.

This paper extends the concepts of SDF for analysis of signals on a two-dimensional domain to facilitate feature extraction directly from the scale-shift wavelet domain without any need for non-unique conversion to a one-dimensional sequence. The proposed method is validated on field data from seismic sensors that monitor the infiltration of humans, light vehicles and animals for border security.

★ This work has been supported in part by the U.S. Army Research Laboratory and the U.S. Army Research Office under Grant No. W911NF-07-1-0376. Any opinions, findings and conclusions or recommendations expressed in this publication are those of the authors and do not necessarily reflect the views of the sponsoring agencies.

†Department of Mechanical Engineering, The Pennsylvania State University, University Park, PA 16802, USA.

‡U.S. Army Research Laboratory, Adelphi, MD 20783, USA.

II. Problem Description and Formulation

This paper focuses on the problem of detection and classification of different targets (e.g., humans, animals, and vehicles), where seismic sensors are used to capture the respective characteristic signatures. For example, in the movement of a human or an animal across the ground, oscillatory motions of the body appendages provide the respective characteristic signature. The seismic data used in this analysis were collected by three-axial geophones from a test field on a wash (i.e., the dry bed of an intermittent creek) full of small granular gravel. During multiple field tests, sensor data were collected for several scenarios that consisted of targets walking along an approximately 150 meters long trail, and returning along the same trail to the starting point. Figure 1 illustrates the data collection scenario.

The targets consisted of people (e.g., male and female humans), animals (e.g., donkeys, mules, and horses), and all-terrain vehicles (ATVs). The humans walked alone and in groups with and without backpacks; the animals were led by their human handlers and they made runs with and without payloads; and the ATVs moved at different speeds (e.g., 5 mph and 10 mph). There were three sensor sites, each equipped with acoustic and seismic sensors. The seismic sensors were buried six inches deep underneath the soil surface. All targets passed by the sensor sites at a distance of approximately 5 meters. Signals from the seismic sensors were acquired at a sampling frequency of 10 KHz.

The tree structure in Fig. 2 shows how the detection and classification problem is formulated. In the detection stage, the pattern classifier detects the presence of a moving target against the null hypothesis of no target present; in the classification stage, the pattern classifier discriminates among different targets. While the detection system should be robust to reduce the false alarm rates, the classification system must be sufficiently sensitive to discriminate between different classes of targets with high fidelity. In this context, feature extraction plays an important role in target detection and classification because the performance of the classifier largely depends on the quality of the extracted features.

In the classification stage, there are multiple classes (i.e., humans, animals, and vehicles); and the signature of the vehicles is distinct from those of the other two classes. Therefore, this problem is formulated into a two-layer classification procedure. A binary classification is first performed to detect

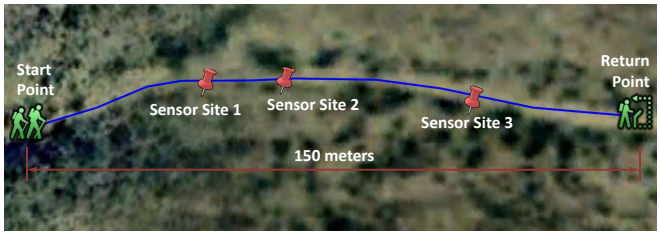

Fig. 1. An illustration of the test scenario with three sensor sites

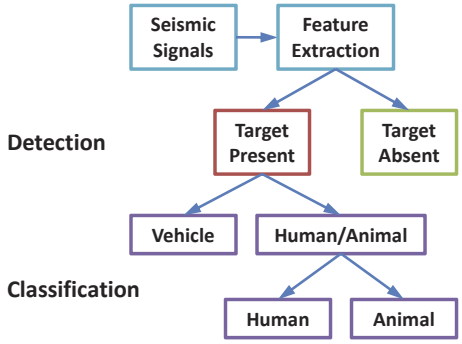

Fig. 2. Tree structure formulation of the detection & classification problem

the presence of a target and then to identify whether the target is a vehicle or a human/animal. Upon recognizing the target as a human/animal, another binary classification is performed to determine the specific class.

III. Symbolic Dynamics and Encoding

While the details of SDF have been reported for analysis of time series data [7][9], this section briefly reviews the underlying concepts of symbolic dynamic filtering (SDF) for feature extraction from sensor time series.

A. Transformation of Time Series to Wavelet Domain

This section presents the procedure for generation of wavelet images from observed sensor time series data for construction of symbolic representations of the underlying dynamics. A crucial step in SDF is partitioning of the phase space for symbol sequence generation. Various partitioning techniques have been suggested in literature for symbol generation, and a brief review is given in [9].

In wavelet-based partitioning, a time series is first transformed to the wavelet domain, where wavelet coefficients are generated at different time shifts and scales. The choice of the wavelet basis function and wavelet scales depends on the time-frequency characteristics of individual signals.

For every wavelet, there exists a certain frequency called the center frequency F_c that has the maximum modulus in the Fourier transform of the wavelet. The pseudo-frequency f_p of the wavelet at a particular scale α is given by the following formula:

$$f_p = \frac{F_c}{\alpha \ \Delta t}, \tag{1}$$

where Δt is the sampling interval, and the scales are calculated as follows:

$$\alpha^i = \frac{F_c}{f_p^i \ \Delta t} \tag{2}$$

where $i = 1, 2, ...,$ and f_p^i are the frequencies that are obtained by choosing the locally dominant frequencies in the Fourier transform.

Figure 3 shows an illustrative example of transformation of the time series (Fig. 3(a)) to a (two-dimensional) wavelet image (Fig. 3(b)). The amplitudes of the wavelet coefficients

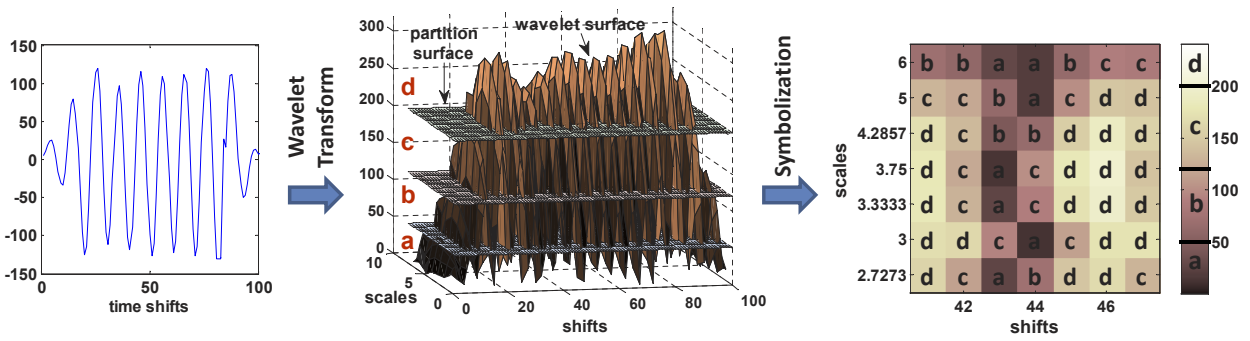

(a) Sensor time series data (b) Partition of the wavelet coefficients (c) Symbolized wavelet image (a section)

Fig. 3. Symbol image generation via wavelet transform of the sensor time series data and partition of the wavelet surface in ordinate direction

over the scale-shift domain are plotted as a surface. Subsequently, symbolization of this wavelet surface leads to the formation of a symbolic image as shown in Fig. 3(c).

B. Symbolization of Wavelet Surface Profiles

This section presents partitioning of the wavelet surface profile, as shown in Fig. 3(b), which is generated by the coefficients over the two-dimensional scale-shift domain, for construction of the symbolic image in Fig. 3(c). The $x-y$ coordinates of the wavelet surface profiles denote the shifts and the scales respectively, and the z-coordinate denotes the pixel values of wavelet coefficients (i.e., the surface height).

The wavelet surface profiles are partitioned such that the ordinates between the maximum and minimum of the coefficients along the z-axis are divided into regions by different planes parallel to the $x-y$ plane. For example, if the alphabet is chosen as $\Sigma = \{a, b, c, d\}$, i.e., $|\Sigma| = 4$, then three partitioning planes divide the ordinate (i.e., z-axis) of the surface profile into four mutually exclusive and exhaustive regions, as shown in Figure 3 (b). These disjoint regions form a partition, where each region is labeled with one symbol from the alphabet Σ. If the intensity of a pixel is located in a particular region, then it is coded with the symbol associated with that region. As such, a symbol from the alphabet Σ is assigned to each pixel corresponding to the region where its intensity falls. Thus, the two-dimensional array of symbols, called *symbol image*, is generated from the wavelet surface profile, as shown in Figure 3 (c).

The surface profiles are partitioned by using either the maximum entropy partitioning (MEP) or the uniform partitioning (UP) methods [10]. If the partitioning planes are separated by equal-sized intervals, then the partition is called the *uniform partitioning* (UP). Intuitively, it is more reasonable if the information-rich regions of a data set are partitioned finer and those with sparse information are partitioned coarser. To achieve this objective, the *maximum entropy partitioning* (MEP) method has been adopted such that the entropy of the generated symbols is maximized. In general, the choice of alphabet size depends on specific data set. The partitioning of wavelet surface profiles to generate symbolic representations enables robust feature extraction, and symbolization also significantly reduces the memory requirements.

For the purpose of pattern classification, the reference data set is partitioned with alphabet size $|\Sigma|$ and is subsequently kept constant. In other words, the structure of the partition is fixed at the reference condition and this partition serves as the reference frame for subsequent data analysis [7].

C. Conversion from Symbol Image to State Image

For analysis of (one-dimensional) time series, the states of a PFSA represent different combinations of blocks of symbols on the symbol sequence and the edges represent the transition probabilities between these blocks [7]. Therefore, for analysis of (one dimensional) time series, the 'states' denote all possible symbol blocks (i.e., words) within a window of certain length. Let us now extend the notion of 'states' for analysis of wavelet surface profiles via construction of a '*state image*' from a '*symbol image*'.

Definition 3.1: (*State*) Let $\mathcal{W} \subset \mathcal{H}$ be a two-dimensional window of size $(\ell \times \ell)$ and its size is denoted as $|\mathcal{W}| = \ell^2$. Then, the state of a symbol block formed by the window $\mathcal{W}$ is defined as the configuration $q{=}S_\Sigma\big(\mathcal{W}\big)$.

Let the set of all possible states in a window $\mathcal{W} \subset \mathcal{H}$ be denoted as $\mathcal{Q} \triangleq \{q_1, q_2, ..., q_{|\mathcal{Q}|}\}$, where $|\mathcal{Q}|$ is the number of (finitely many) states. Let us denote $\mathcal{W}_{i,j} \subset \mathcal{H}$ to be the window where (i, j) represents the coordinates of the top-left corner pixel of the window. In this notation, $q_{i,j}{=}S_\Sigma\big(\mathcal{W}_{i,j}\big)$ denotes the state at pixel $(i, j) \in \mathcal{H}$. Thus, every pixel $(i, j) \in \mathcal{H}$ corresponds to a particular state $q_{i,j} \in \mathcal{Q}$ on the image. Then, $|\mathcal{Q}|$ is bounded above as $|\mathcal{Q}| \leq |\Sigma|^{|\mathcal{W}|}$; the inequality is due to the fact that some of the states might have zero probability of occurrence.

Every pixel in the image $\mathcal{H}$ is mapped to a state (i.e., a two-dimensional word or block of symbols), excluding the pixels that lie at the periphery depending on the window size. Figure 4 shows an illustrative example of the transformation of a *symbol image* to the *state image* based on a sliding window $\mathcal{W}$ of size (2×2). This concept of state formation facilitates capturing of long range dynamics (i.e., word to word interactions) on a symbol image.

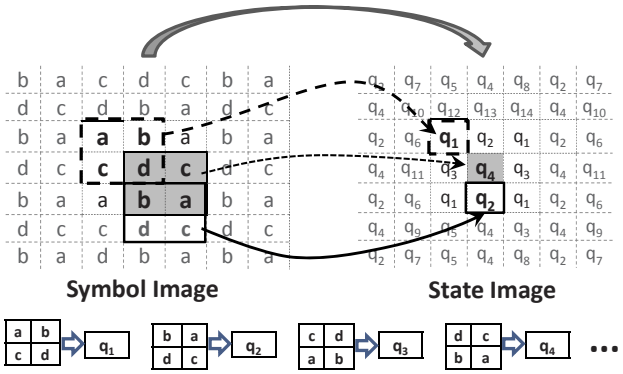

Fig. 4. Conversion of the symbol image to the state image

In general, a large number of states would require a high computational capability and hence might not be feasible for real-time applications. The number of states, $|\mathcal{Q}|$, increases with the window size $|\mathcal{W}|$ and the alphabet size $|\Sigma|$. For example, if $\ell = 2$ and $|\Sigma| = 4$, then the total number of states are $|\mathcal{Q}| \leq |\Sigma|^{\ell^2} = 256$. Therefore, for computational efficiency, it is necessary to compress the state set $\mathcal{Q}$ to an effective smaller set $\mathcal{O} \triangleq \{o_1, o_2, ..., o_{|\mathcal{O}|}\}$ that enables mapping of two or more different configurations in a window $\mathcal{W}$ to a single state. State compression must preserve sufficient information as needed for pattern classification, albeit possibly lossy coding of the wavelet surface profile.

A probabilistic state compression method is employed, which chooses m most probable symbols from each state as a representation of that particular state. In this method, each state consisting of $\ell \times \ell$ symbols is compressed to a word of length $m < \ell^2$ symbols by choosing the top m symbols that have the highest probability of occurrence. This procedure reduces the state set $\mathcal{Q}$ to an effective set $\mathcal{O}$, where the total number of compressed states is given as: $|\mathcal{O}| = |\Sigma|^m$. For example, if $|\Sigma| = 4$, $|\mathcal{W}| = 4$ and $m = 2$, then the state compression reduces the total number of states to $|\mathcal{O}| = |\Sigma|^m = 16$ instead of 256.

The choice of $|\Sigma|$, ℓ and m depends on specific applications and noise level as well as the available computational power, and is made by an appropriate tradeoff between robustness to noise and capability to detect small changes. For example, a large alphabet may be noise-sensitive while a small alphabet may miss the information of signal dynamics.

D. Construction of PFSA and Pattern Classification

A probabilistic finite state automaton (PFSA) is constructed such that the states of the PFSA are the elements of the compressed state set $\mathcal{O}$ and the edges are the transition probabilities between these states. The transition probabilities are defined as:

$$\wp(o_k|o_l) = \frac{N(o_l, o_k)}{\sum_{k'=1,2,...,|\mathcal{O}|} N(o_l, o_{k'})} \quad \forall\ o_l, o_k \in \mathcal{O} \qquad (3)$$

where $N(o_l, o_k)$ is the total count of events when o_k occurs adjacent to o_l in the direction of motion. A transition from the state o_l to the state o_k occurs if o_k lies adjacent to o_l in the positive direction of motion. Subsequently, the counter moves to the right and to the bottom (row-wise) to cover the entire state image, and the transition probabilities $\wp(o_k|o_l)$, $\forall\ o_l, o_k \in \mathcal{O}$ are computed using Eq. (3). Therefore, for every state on the state image, all state-to-state transitions are counted, as shown in Figure 5. For example, the dotted box in the bottom-right corner contains three adjacent pairs, implying the transitions $o_1 \rightarrow o_2$, $o_1 \rightarrow o_3$, and $o_1 \rightarrow o_4$ and the corresponding counter of occurrences $N(o_1, o_2)$, $N(o_1, o_3)$ and $N(o_1, o_4)$, respectively, are increased by one. This procedure generates the state-transition probability matrix of the PFSA given as:

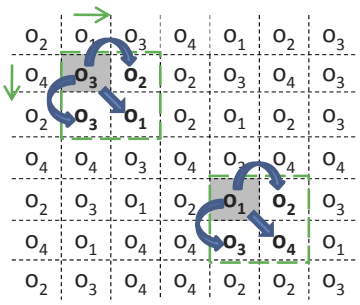

Fig. 5. An example of feature extraction from the state image

$$\Pi = \begin{bmatrix} \wp(o_1|o_1) & \dots & \wp(o_{|\mathcal{O}|}|o_1) \\ \vdots & \ddots & \vdots \\ \wp(o_1|o_{|\mathcal{O}|}) & \dots & \wp(o_{|\mathcal{O}|}|o_{|\mathcal{O}|}) \end{bmatrix} \qquad (4)$$

where $\Pi \equiv [\pi_{jk}]$ with $\pi_{jk} = \wp(o_k|o_j)$. Note: $\pi_{jk} \geq 0\ \forall j, k \in \{1, 2, ...|\mathcal{O}|\}$ and $\sum_k \pi_{jk} = 1\ \forall j \in \{1, 2, ...|\mathcal{O}|\}$.

In order to extract a low-dimensional feature vector, the stationary state probability vector $\mathbf{p}$ is obtained as the left eigenvector corresponding to the unity eigenvalue of the stochastic transition matrix Π. The state probability vectors $\mathbf{p}$ serve as the '*feature vectors*' and are generated from different data sets from the corresponding state transition matrices. These feature vectors are denoted as '*patterns*' in this paper.

IV. Results of Field Data Analysis

Field data were collected in the scenario illustrated in Fig. 1. Multiple data runs were made to collect data sets of all three classes, i.e., human, vehicle, and animal. Each data set, sampled at a sampling frequency of 10 kHz, has 2.5×10^5 data points that correspond to 25 seconds of experimentation time. In order to test the capability of the proposed algorithm in target detection, another group of data were collected with no target present. The problem of target detection is then formulated as a binary pattern classification, where the no target present data are considered as one class, and the others with target present (i.e., human, animal, or vehicle) are considered to belong to the other class. The data sets, collected by the channel of seismic sensors that are orthogonal to the ground surface, are used for target detection

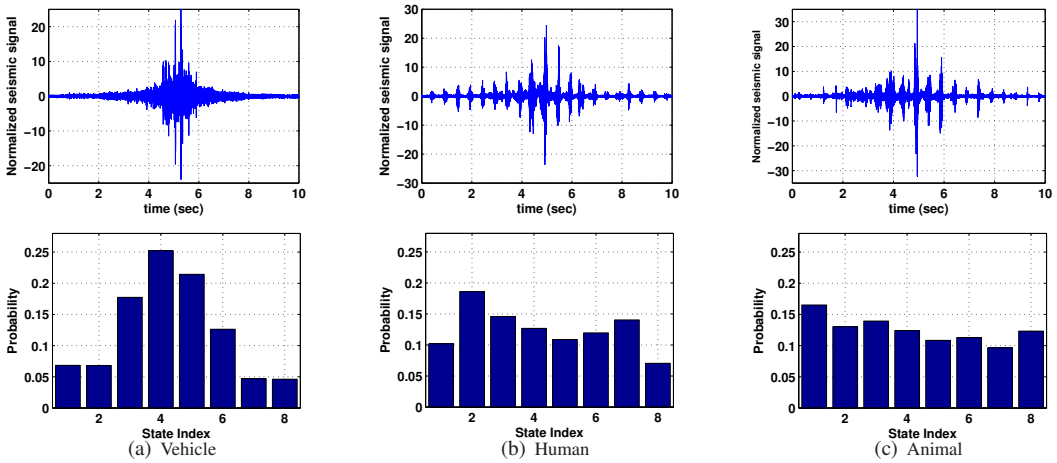

(a) Vehicle (b) Human (c) Animal

Fig. 6. Examples of seismic sensor measurements (top) and ensemble mean of the feature vectors extracted by SDF of the three classes (bottom)

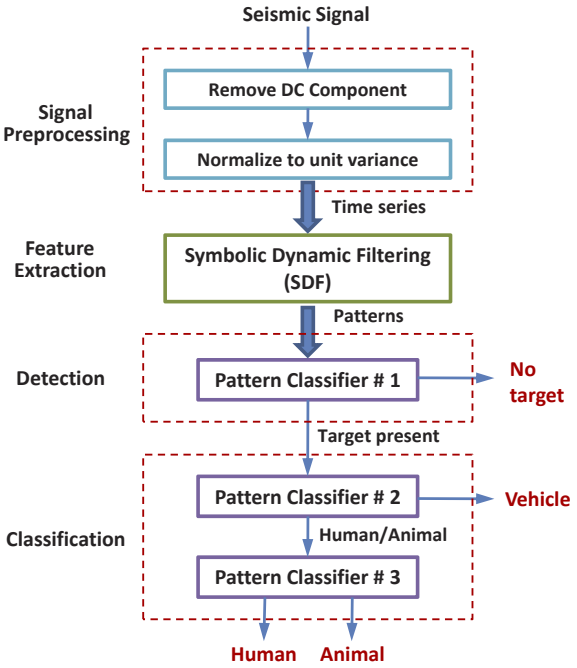

Fig. 7. Flow chart of the problem of target detection and classification

and classification. For computational efficiency, the original seismic data were downsampled by a factor of 10, and only a part of the entire data points in each data set has been used.

Figure 7 depicts the flow chart of the proposed detection and classification algorithm that is constructed based on the theories of symbolic dynamic filtering (SDF) and support vector machine (SVM) [11]. The proposed algorithm consists of four steps, namely, signal preprocessing, feature extraction, detection, and classification, as shown in Fig. 7.

In the signal preprocessing step, the DC component of the original signal is eliminated, and the signal is normalized to unit variance. The signal amplitude of a vehicle passing by far away may be similar to that of a pedestrian passing by at close distance due to the fact that the SNR decreases rapidly with the distance between the sensor and the target. The normalization of all signals to unit variance makes the pattern classifier independent of the signal amplitude and any discrimination should be solely texture-dependent.

In the feature extraction step, SDF captures the signatures of the data, normalized to be zero-mean unit-variance sensor time-series, for representation as low-dimensional feature vectors. Based on the spectral analysis of the ensemble of seismic data at hand, a series of pseudo-frequencies from the 1-10 Hz bands have been chosen to generate the scales for wavelet transform, because these bands contain a very large part of the footstep energy [6]. Upon generation of the scales, continuous wavelet transforms (CWT) are performed with $db7$ mother wavelet since it matches the shape of seismic signals very well. A maximum-entropy wavelet surface partitioning is then performed. Selection of the alphabet size $|\Sigma|$ depends on the characteristics of the signal, where a small alphabet is robust against noise and environmental variation and a large alphabet has increased discriminant power for identifying different objects. The same alphabet is used for both target detection and classification and the issues of alphabet size optimization and data set partitioning are not addressed in this paper. The execution of the code takes less than 0.5 second for SDF to process a data set of 2.5×10^4 points with the following choice of parameters: alphabet size $|\Sigma| = 8$, number of scales $|\alpha| = 5$, window length $\ell = 2$ and number of most probable symbol $m = 1$ (see Section III-C). Figure 6 shows the normalized seismic sensor signals and the corresponding feature vectors extracted by SDF of the three classes of targets.

The next step is to perform pattern classification on the feature vectors. Three classifiers are needed, as seen in the flow chart of Fig. 7: one for target detection to decide whether a target is present or not, and the other two are for target identification. All classifiers are implemented by support vector machines (SVMs). The SVM generates a hyperplane to maximize the margin and to minimize the

classification errors between feature vectors of the training data. If the data sets are not linearly separable, the SVM may allow for some of the training points to be on the wrong side of the hyperplane through inclusion of slack variables [11]. In this paper, *polynomial* kernels are used in all three SVMs since the feature vectors are no longer linearly separable. In the testing stage, the feature vectors are generated from SDF with unknown class labels and are then separated by the hyperplane obtained in the training stage. The SVM yields a binary output as the class labels of the testing data.

Following Fig. 7, the tested cases are listed below:

1) Detection of target presence against target absence
2) Pairwise classification of target type, i.e., *Vehicle vs. Human/Animal*, and *Human vs. Animal*.

Results of the leave-one-out cross-validation [11] are summarized in Table I, where the second column describes the scenarios and the third column shows the classification results in the format: accuracy $\left(\frac{\#\ \text{of correct classifications}}{\#\ \text{of total data sets}}\right)$. The ground truth is: 50 cases of target present and 18 cases of no target present. Out of these 50 target-present cases, there are 9 vehicles, 17 humans, and 24 animals.

The top part of Table I shows the results of target detection at 100% accuracy. This is followed by the results of target classification at overall 90.0% accuracy, where a two-layer classification procedure has been used. Since the total number of vehicle data sets is small, the result of vehicle discrimination is slightly low at 88.9% accuracy, which is expected to improve for larger vehicle data sets. In total, there are five errors in target classification, where three errors are from "Vehicle vs. Human/Animal" tests, and the remaining two errors are from "Human vs. Animal" test. An error in the "Human vs. Animal" test is the same as that in "Vehicle vs. Human/Animal" test, so it is counted only once.

TABLE I
LEAVE-ONE-OUT CROSS-VALIDATION RESULTS

Detection	Target Present vs. No Target		
	Target Detected	100.0%	(50/50)
	No Target	100.0%	(18/18)
	Total Detection Rate	**100.0%**	(68/68)
Classification	Vehicle vs. Human/Animal		
	Vehicle Discrimination	88.9%	(8/9)
	Human/Animal Discrimination	95.1%	(39/41)
	Subtotal	**94.0%**	(47/50)
	Human vs. Animal		
	Human Discrimination	94.1%	(16/17)
	Animal Discrimination	91.7%	(22/24)
	Subtotal	**92.7%**	(38/41)
	Total Classification Rate	**90.0%**	(45/50)

V. SUMMARY, CONCLUSIONS AND FUTURE WORK

This paper presents a symbolic feature extraction method for target detection and classification, where the features are extracted as statistical patterns by symbol-based models of wavelet images that are generated from time series of seismic sensors. By an appropriate selection of wavelet basis and scale range, the continuous-wavelet-transformed signal is denoised relative to the original time-domain signal. In this way, the symbolic images generated from wavelet coefficients capture the signal characteristics with larger fidelity than those obtained directly from the time-domain signal. The symbolic images are then modeled using probabilistic finite state automata (PFSA) that, in turn, generate low-dimensional statistical patterns, treated as feature vectors. A distinct advantage of the proposed method is that the low-dimensional feature vectors can be computed in-situ and communicated in real time over a limited-bandwidth wireless sensor network with limited-memory nodes.

The feature extraction method has been validated on a set of field data for target detection and classification. The results generated from this set of field data show: (i) absence of any false alarms and missed detection of targets, and (ii) high accuracy in discriminating the types of targets.

While there are many research issues that need to resolved before exploring commercial applications of the proposed method, the following topics are under active research:

- Optimization of the partition scheme for symbolization;
- Enhancement of target detection and classification performance by fusion of multimodal sensor signals.

REFERENCES

[1] G. L. Goodman, "Detection and classification for unattended ground sensors.," in *Proceedings of Information Decision and Control 99*, pp. 419–424, 1999.

[2] Y. Tian and H. Qi, "Target detection and classification using seismic signal processing in unattended ground sensor systems," in *International Conference on Acoustics Speech and Signal Processing*, 2002.

[3] J. Altmann, "Acoustic and seismic signals of heavy military vehicles for co-operative verification," *Journal of Sound and Vibration*, vol. 273, no. 4-5, pp. 713 – 740, 2004.

[4] G. P. Succi, D. Clapp, R. Gampert, and G. Prado, "Footstep detection and tracking," in *Unattended Ground Sensor Technologies and Applications III*, vol. 4393, pp. 22–29, SPIE, 2001.

[5] J. Lacombe *et al.*, "Seismic detection algorithm and sensor deployment recommendations for perimeter security," in *Unattended Ground, Sea, Air Sensor Technologies & Applications VIII*, vol. 6231, SPIE, 2006.

[6] K. M. Houston and D. P. McGaffigan, "Spectrum analysis techniques for personnel detection using seismic sensors," in *Unattended Ground Sensor Technologies & Applications V*, vol. 5090, pp. 162–173, SPIE.

[7] A. Ray, "Symbolic dynamic analysis of complex systems for anomaly detection," *Signal Processing*, vol. 84, no. 7, pp. 1115–1130, 2004.

[8] C. Rao, A. Ray, S. Sarkar, and M. Yasar, "Review and comparative evaluation of symbolic dynamic filtering for detection of anomaly patterns," *Signal, Image, Video Processing*, vol. 3, pp. 101–114, 2009.

[9] X. Jin, K. Mukherjee, S. Gupta, and A. Ray, "Wavelet-based feature extraction using probabilistic finite state automata for pattern classification," *Pattern Recognition*, vol. 44, pp. 1343–1356, July 2011.

[10] V. Rajagopalan and A. Ray, "Symbolic time series analysis via wavelet-based partitioning," *Signal Processing*, vol. 86, no. 11, pp. 3309–3320, Nov 2006.

[11] C. M. Bishop, *Pattern Recognition and Machine Learning*. Springer, 2006.